

See discussions, stats, and author profiles for this publication at: <https://www.researchgate.net/publication/6892540>

# Cooperative Hydration of Pyruvic Acid in Ice

ARTICLE in JOURNAL OF THE AMERICAN CHEMICAL SOCIETY · JULY 2006

Impact Factor: 12.11 · DOI: 10.1021/ja062039v · Source: PubMed

---

CITATIONS

12

---

READS

31

## 4 AUTHORS:



[Marcelo I. Guzman](#)

University of Kentucky

60 PUBLICATIONS 693 CITATIONS

SEE PROFILE



[Lea Hildebrandt Ruiz](#)

University of Texas at Austin

29 PUBLICATIONS 1,205 CITATIONS

SEE PROFILE



[Agustin J Colussi](#)

California Institute of Technology

214 PUBLICATIONS 4,174 CITATIONS

SEE PROFILE



[Michael R. Hoffmann](#)

California Institute of Technology

376 PUBLICATIONS 29,578 CITATIONS

SEE PROFILE

## Cooperative Hydration of Pyruvic Acid in Ice

Marcelo I. Guzmán, Lea Hildebrandt, Agustín J. Colussi,\* and Michael R. Hoffmann

*Contribution from the W. M. Keck Laboratories, California Institute of Technology,  
Pasadena, California 91125*

Received March 24, 2006; E-mail: ajcoluss@caltech.edu

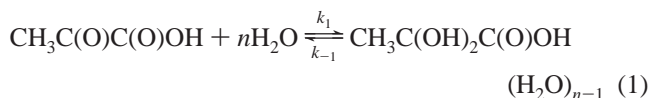
**Abstract:** About  $3.5 \pm 0.3$  water molecules are still involved in the exothermic hydration of 2-oxopropanoic acid (PA) into its monohydrate (2,2-dihydroxypropanoic acid, PAH) in ice at 230 K. This is borne out by thermodynamic analysis of the fact that  $Q_H(T) = [\text{PAH}]/[\text{PA}]$  becomes temperature independent below  $\sim 250$  K (in chemically and thermally equilibrated frozen  $0.1 \leq [\text{PA}]/M \leq 4.6$  solutions in  $\text{D}_2\text{O}$ ), which requires that the enthalpy of PA hydration ( $\Delta H_H \sim -22 \text{ kJ mol}^{-1}$ ) be balanced by a multiple of the enthalpy of ice melting ( $\Delta H_M = 6.3 \text{ kJ mol}^{-1}$ ). Considering that: (1) thermograms of frozen PA solutions display a single endotherm, at the onset of ice melting, (2) the sum of the integral intensities of the  $^1\delta_{\text{PAH}}$  and  $^1\delta_{\text{PA}}$  methyl proton NMR resonances is nearly constant while, (3) line widths increase exponentially with decreasing temperature before diverging below  $\sim 230$  K, we infer that PA in ice remains cooperatively hydrated within interstitial microfluids until they vitrify.

### Introduction

The fluid films wetting ice support important chemical, biochemical, and environmental processes.<sup>1–7</sup> The existence of subeutectic aqueous solutions,<sup>8–10</sup> of unfrozen water bound to mesoscopic objects, such as membranes and macromolecules, in the presence of ice,<sup>1–3,11,12</sup> and the premelting,<sup>13–16</sup> and prefreezing,<sup>17</sup> of pure substances and mixtures reveal that interfaces differ significantly from bulk phases and can support novel phenomena.

Upon freezing, solutes largely ( $>99.9\%$ ) accumulate in the unfrozen portion,<sup>6,8,18–24</sup> but the marginal and selective incorporation of ions into ice induces sizable polarizations that are

ultimately relieved by interfacial proton migration.<sup>25–27</sup> Chemical reaction rates and equilibria in frozen solutions are therefore expected to be enhanced by trivial concentration effects,<sup>28</sup> generally retarded by the prevalent low temperatures,<sup>26,29</sup> and potentially affected by the acidity changes ensuing freezing.<sup>30</sup> Although solute solvation plays a crucial role in chemistry, the likelihood of water exchange and the extent of solute dehydration in ice interfacial layers, vis-à-vis the decreased activity of water at sub-freezing temperatures, remains largely unexplored. The hydration of pyruvic acid (PA) into its *gem*-diol, 2,2-dihydroxypropanoic acid (PAH), reaction 1:



whose equilibrium constant,  $K_H$ :

$$K_H = \frac{[\text{CH}_3\text{C}(\text{OH})_2\text{COOH}(\text{H}_2\text{O})_{n-1}]}{[\text{CH}_3\text{COCO}(\text{OH})] a_w^n} = \frac{Q_H}{a_w^n} \quad (2)$$

(where  $a_w$  is the water activity) is known to involve more than the stoichiometric ( $n = 1$ ) amount of water in fluid solutions,<sup>31–35</sup> should be a sensitive probe of water availability in frozen

- (1) Yang, C.; Sharp, K. A. *Proteins* **2005**, 59, 266.
- (2) Wolfe, J.; Bryant, G.; Koster, K. L. *CryoLett.* **2002**, 23, 157.
- (3) Fukuhara, M.; Kokuta, A. *CryoLett.* **2005**, 26, 251.
- (4) Karcher, B.; Koop, T. *Atmos. Chem. Phys.* **2005**, 5, 703.
- (5) Hamdami, N.; Monteau, J. Y.; Le Bail, A. *J. Food Eng.* **2004**, 62, 373.
- (6) Dash, J. G.; Fu, H. Y.; Wettlaufer, J. S. *Rep. Prog. Phys.* **1995**, 58, 115.
- (7) Boxe, C. S.; Colussi, A. J.; Hoffmann, M. R.; Perez, I. M.; Murphy, J. G.; Cohen, R. C. *J. Phys. Chem. A* **2006**, 110, 3578.
- (8) Cho, H.; Shepson, P. B.; Barrie, L. A.; Cowin, J. P.; Zavery, R. *J. Phys. Chem.* **2002**, 106, 11226.
- (9) Richardson, C. J. *Glaciol.* **1976**, 17, 507.
- (10) Boxe, C. S.; Colussi, A. J.; Hoffmann, M. R.; Tan, D.; Mastromarino, J.; Sandholm, S. T.; Davies, D. D. *J. Phys. Chem. A* **2003**, 107, 11409.
- (11) Schreiber, A.; Ketelsen, I.; Findenegg, G. H. *Phys. Chem. Chem. Phys.* **2001**, 3, 1185.
- (12) Yeh, Y.; Feeney, R. E. *Chem. Rev.* **1996**, 96, 601.
- (13) Wettlaufer, J. S.; Worster, M. G. *Annu. Rev. Fluid Mech.* **2006**, 38, 427.
- (14) Henson, B. F.; Voss, L. F.; Wilson, K. R.; Robinson, J. M. *J. Chem. Phys.* **2005**, 123, 144707.
- (15) Henson, B. F.; Robinson, J. M. *Phys. Rev. Lett.* **2004**, 92, 246107.
- (16) Ewing, G. E. *J. Phys. Chem. B* **2004**, 108, 15953.
- (17) Colussi, A. J.; Hoffmann, M. R.; Tang, Y. *Langmuir* **2000**, 16, 5213.
- (18) Jungwirth, P.; Vrbka, L. *Phys. Rev. Lett.* **2005**, 95, 148501.
- (19) Angell, C. A. Supercooled water. In *Water, A Comprehensive Treatise*; Franks, F., Ed.; Plenum: New York, 1982; Vol. 7.
- (20) Doppenschmidt, A.; Butt, H.-J. *Langmuir* **2000**, 16, 6709.
- (21) Petrenko, V. F.; Whitworth, R. W. *The Physics of Ice*; Oxford University Press: Oxford, 1999.
- (22) Ruzicka, R.; Barakova, L.; Klan, P. *J. Phys. Chem. B* **2005**, 109, 9346.
- (23) Heger, D.; Jirkovský, J.; Klán, P. *J. Phys. Chem. A* **2005**, 109, 6702.
- (24) Workman, E. J.; Reynolds, S. E. *Phys. Rev.* **1950**, 78, 1950.

- (25) Finnegan, W.; Pitter, R.; Hinsvark, B. *J. Coll. Interfac. Sci.* **2001**, 242, 373.
- (26) Takenaka, N.; Ueda, A.; Maeda, Y. *Nature* **1992**, 358, 736.
- (27) Bronshteyn, V. L.; Chernov, A. A. *J. Cryst. Growth* **1991**, 112, 129.
- (28) Pincock, R. E. *Acc. Chem. Res.* **1969**, 2, 97.
- (29) Takenaka, N.; Ueda, A.; Daimon, T.; Bandow, H.; Dohmaru, T.; Maeda, Y. *J. Phys. Chem.* **1996**, 100, 13874.
- (30) Robinson, C.; Boxe, C. S.; Guzman, M. I.; Colussi, A. J.; Hoffmann, M. R. *J. Phys. Chem. B* **2006**, 110, 7613.
- (31) Pocker, Y.; Meany, J. E.; Nist, B. J.; Zadorojn, C. *J. Phys. Chem.* **1969**, 73, 2879.
- (32) Knoche, W.; Lopez-Quintela, M. A.; Weiffen, J. *Ber. Bunsen-Ges. Phys. Chem.* **1985**, 89, 1047.

media.<sup>36–39</sup> Here, we report magic angle spinning nuclear magnetic resonance (MAS NMR) and differential scanning calorimetry (DSC) experiments in fluid and frozen pyruvic acid aqueous solutions down to 230 K that provide quantitative information on the physicochemical properties of the quasi-liquid layer.

### Experimental Section

MAS  $^1\text{H}$  NMR spectra of frozen PA (Aldrich 98.0%, doubly distilled under vacuum) solutions in  $\text{D}_2\text{O}$  (Alfa 99.8%,  $T_f = 277.0$  K), contained in capped  $\text{ZrO}_2$  rotors (100  $\mu\text{L}$ , 4-mm internal diameter) spun at  $3.2 \pm 0.1$  kHz, were acquired with a Bruker ARX500 spectrometer equipped with a triple resonance 4-mm probe and cavity temperature control. Spinning samples were allowed to equilibrate for at least 20 min at each temperature prior to spectral scans. Spectra were scanned over consecutive cooling and warming sequences spanning the entire temperature range, or over  $\pm 2$  K cycles about specific temperatures. Probe temperatures were calibrated using reported  $^1\delta_{\text{OH}} - ^1\delta_{\text{CH}_3}$  vs.  $T$  data for methanol down to 228 K.<sup>40</sup>  $^1\text{H}$  NMR spectra of fluid solutions were recorded with a Varian Unity 500 Plus spectrometer. Thermal studies on aqueous PA samples (200  $\mu\text{L}$ ) were performed in a Netzsch STA 449 differential scanning calorimeter (DSC) calibrated with neat  $\text{H}_2\text{O}$  and  $\text{D}_2\text{O}$  standards.

### Results and Discussion

The  $^1\text{H}$  NMR spectrum of neat PA(l) at 298 K shows resonances at 8.70 and 2.53 ppm (relative to TMS), which are assigned to acidic and methyl protons, respectively. The  $^1\text{H}$  NMR spectrum of PA in frozen aqueous solution displays, in contrast, two methyl bands: one at  $^1\delta = 1.54$  ppm, which corresponds to PAH, and a less intense one at  $^1\delta = 2.38$  ppm, the correlate of the 2.53 ppm PA band (Figure 1). The positions of the 1.54 and 2.38 bands of PAH and PA slightly shift upfield, whereas their peak intensities and widths change smoothly with decreasing temperature (Figure 1). A single  $^1\delta > 5$  ppm band, which markedly shifts downfield and broadens at lower temperatures (Figure 2), is assigned to mobile water protons<sup>19,41–43</sup> arising from rapid proton exchange between  $[^1\text{H}_4]\text{PA}$  and solvent  $\text{D}_2\text{O}$ . The  $^1\delta$  band of water held in the relatively anhydrous environment of reverse micelles is known to shift, in contrast, upfield.<sup>42,44</sup>

PA and PAH concentrations in aqueous solution are directly proportional to the 2.38 and 1.54 ppm band areas, respectively. Figure 3 shows  $Q_{\text{H}} = [\text{PAH}]/[\text{PA}]$  measurements as function of  $a_{\text{w}}$  (standard state neat water, i.e.,  $x_{\text{w}} = 1$ , 298 K) in aqueous PA solutions of various compositions ( $0.002 \leq x_{\text{PA}} = 1 - x_{\text{w}} \leq 0.87$ ) at 298 K. The two curves in Figure 3 were drawn from present  $Q_{\text{H}}(x_{\text{w}})$  data by: (1) assuming  $a_{\text{w}} = x_{\text{w}}$  throughout or, (2) adopting the  $a_{\text{w}} = a_{\text{w}}(x_{\text{w}})$  values reported for acetic acid

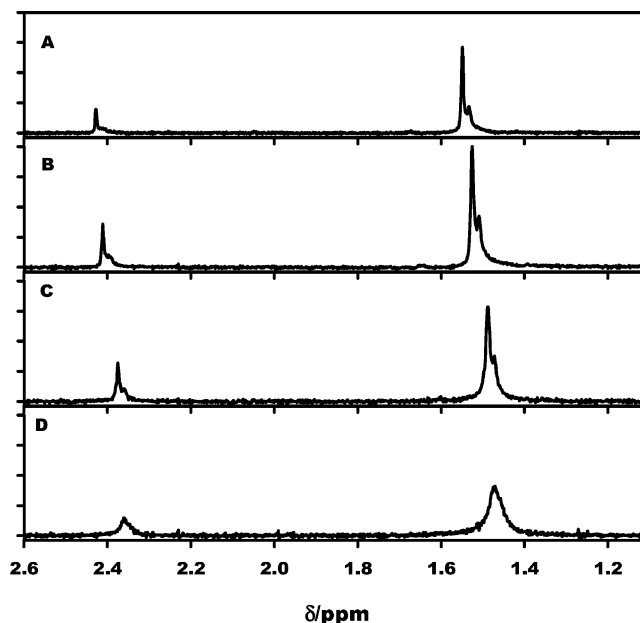


**Figure 1.** MAS  $^1\text{H}$  NMR spectra of frozen 0.1 M pyruvic acid solutions in  $\text{D}_2\text{O}$  at 275.3 (A), 261.3 (B), 250.5 (C), and 239.7 K (D). Signals at  $^1\delta \approx 2.4$  and  $\approx 1.5$  ppm (vs TMS) correspond to methyl protons of pyruvic acid and its gem-diol, respectively.

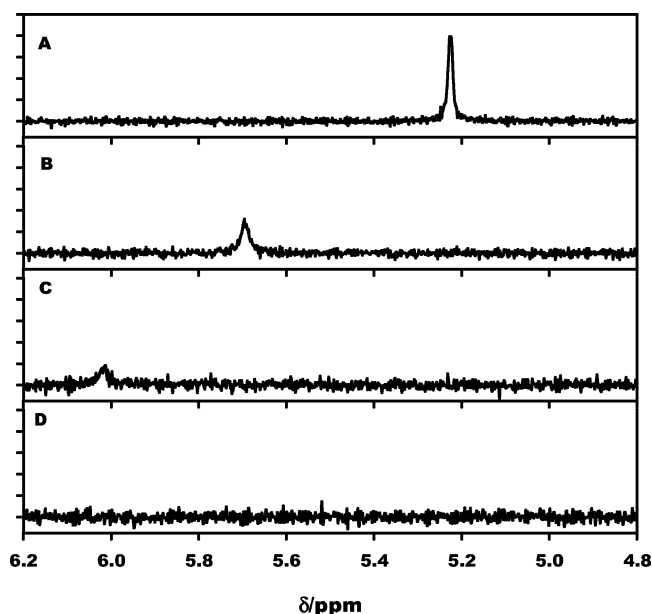


**Figure 2.**  $^1\delta \geq 5$  ppm water NMR signals in frozen 0.1 M pyruvic acid solutions in  $\text{D}_2\text{O}$  under the same conditions of Figure 1.

aqueous solutions. These choices are deemed to bracket the anticipated (positive) deviations of the water activity coefficient,  $\gamma_{\text{w}} = a_{\text{w}}/x_{\text{w}} \geq 1$ , in PA solutions.<sup>45–47</sup> The limiting slopes of the  $\log Q_{\text{H}}$  vs  $\log a_{\text{w}}$  plots of Figure (1) at  $a_{\text{w}} \rightarrow 0$  and  $a_{\text{w}} \rightarrow 1$  correspond, according to eq 2, to  $n_0$  and  $n_1$ , the number of water molecules actually involved in equilibrium (1,  $-1$ ) in concentrated and dilute PA solutions, respectively. We obtain:  $n_0 = 0.9$ ,  $n_1 = 6.2$  for choice (1) above, and  $n_0 = 1.2$ ,  $n_1 = 8.3$  for choice (2). These  $n_1$  values encompass the  $n_1 \approx 6.5$  value

(33) Buschmann, H. J.; Dutkiewicz, E.; Knoche, W. *Ber. Bunsen-Ges. Phys. Chem.* **1982**, *86*, 129.

(34) Buschmann, H. J.; Fuldner, H. H.; Knoche, W. *Ber. Bunsen-Ges. Phys. Chem.* **1980**, *84*, 41.

(35) Menzel, H. M. *Ber. Bunsen-Ges. Phys. Chem.* **1974**, *78*, 89.

(36) Wolfe, S.; Kim, C. K.; Yang, K.; Weinberg, N.; Shi, Z. *J. Am. Chem. Soc.* **1995**, *117*, 4240.

(37) Wolfe, S.; Shi, Z.; Yang, K.; S., R.; Weinberg, N.; Kim, C. K. *Can. J. Chem.* **1998**, *76*, 114.

(38) Hsieh, Y. H.; Weinberg, N.; Yang, K.; Kim, C. K.; Shi, Z.; Wolfe, S. *Can. J. Chem.* **2005**, *83*, 769.

(39) Likar, M. D.; Taylor, R. J.; Fagerness, P. E.; Hiyama, Y.; Robins, R. H. *Pharm. Res.* **1993**, *10*, 75.

(40) Van Geet, A. L. *Anal. Chem.* **1970**, *42*, 679.

(41) Angell, C. A.; Shuppert, J.; Tucker, J. C. *J. Phys. Chem.* **1973**, *77*, 3092.

(42) Wong, M.; Thomas, J. K.; Nowak, T. *J. Am. Chem. Soc.* **1977**, *99*, 4730.

(43) Simorellis, A. K.; Van Horn, W. D.; Flynn, P. F. *J. Am. Chem. Soc.* **2006**, *128*.

(44) Thompson, K. F.; Gierasch, L. M. *J. Am. Chem. Soc.* **1984**, *106*, 3648.

(45) Hansen, R. S.; Miller, F. A.; Christian, S. D. *J. Phys. Chem.* **1955**, *59*, 391.

(46) Clegg, S. L.; Seinfeld, J. H.; Brimblecombe, P. *J. Aerosol Sci.* **2001**, *32*, 713.

(47) Raatikainen, T.; Laaksonen, A. *Atmos. Chem. Phys.* **2005**, *5*, 2475.

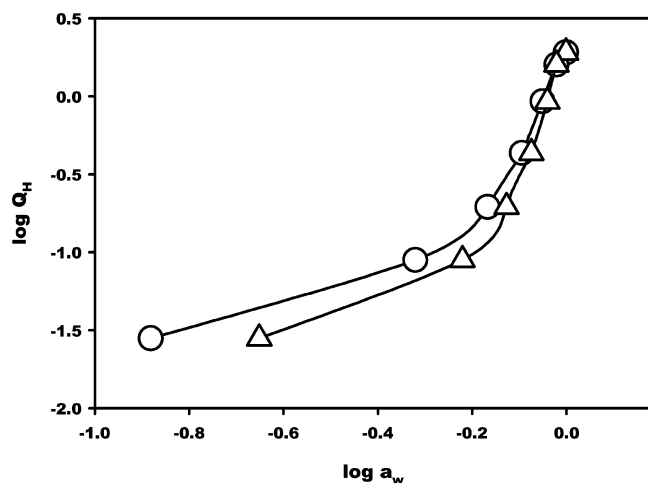


**Figure 3.**  $\log Q_H$  vs.  $\log a_w$  in PA solutions in  $D_2O$  at 298 K. (○)  $\gamma_w = 1$ . (△)  $\gamma_w$  as in acetic acid solutions.<sup>45</sup>

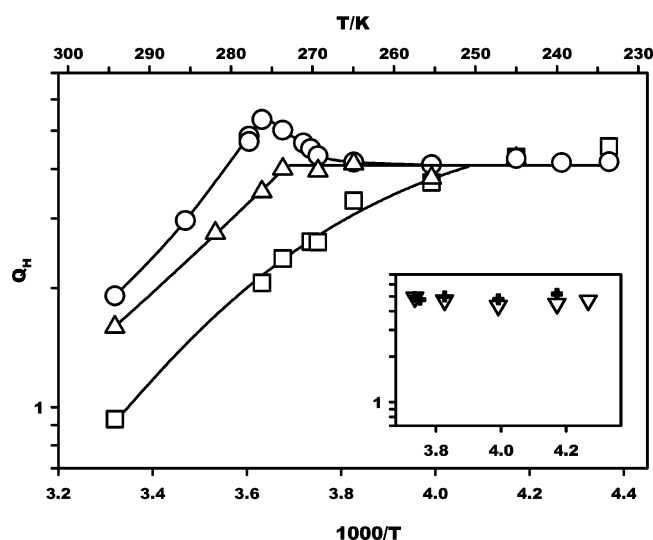


**Figure 4.**  $\log Q_H$  vs.  $1000/T$  in: (○) 0.1 M. (△) 2.32 M. (□) 4.64 M PA solutions in  $D_2O$ . (Inset) (▽) in 0.16 M PA/0.13 M HCl. (+) in 0.16 M PA/0.5 M NaCl.

previously reported for PA hydration in water–dioxane mixtures in the range  $0.6 \leq a_w \leq 1$ .<sup>32</sup> The same report reveals strong deviations at  $a_w \leq 0.6$ , which are consistent with the condition  $n_0 < n_1$ , i.e., with decreased solvation in more concentrated PA solutions. Notice that the  $n \approx 3$  values derived elsewhere from  $\log Q_H$  vs  $\log [H_2O]$  plots are implicitly based on the choice of 1 M water ideal solution at 298 K as standard state,<sup>31</sup> which is not appropriate for correlating the  $Q_H$  vs  $a_w$  dependences above and below the freezing point. It is the activity of pure water, i.e.,  $a_w$  in the molar fraction concentration scale, that is related to the activity of ice, the stable phase, at subfreezing temperatures.

The  $Q_H$  vs.  $T$  data obtained in 0.10, 2.32, and 4.64 M PA solutions above and below their respective freezing points are shown in Figure 4. As expected,  $Q_H$  increases with decreasing temperature in the fluid region in all cases. We obtain  $\Delta H_H = -27.3$  kJ mol<sup>-1</sup> for the 0.1 M PA solution, in excellent agreement with Menzel's data in  $D_2O$  as solvent at 298 K,<sup>35</sup> and  $\Delta H_H = -21.3$  and  $-20.5$  kJ mol<sup>-1</sup> for the 2.32 and 4.64 M PA solutions, respectively. These figures confirm that PAH stability and  $n$  increase with dilution. As a reference, the colligatively depressed freezing temperatures (estimated from the cryoscopic constant of  $D_2O$ ,  $\lambda = 2.01$  K molal<sup>-1</sup>, by

assuming that PA remains largely undissociated) are  $T_f \approx 277.0 - 2.01 [PA] = 276.8, 272.3$ , and  $267.7$  K, for  $[PA] = 0.10, 2.32$ , and  $4.64$  M, respectively. Although these solutions freeze without discontinuities in  $Q_H$ , the slope:  $\partial Q_H / \partial T = \partial (K_1 \times a_w^n) / \partial T$ , reverses its sign at  $T_f$  for the more dilute 0.1 M PA solution. Ultimately, all  $Q_H$ 's asymptotically merge into a common  $Q_H = 4.2 \pm 0.3$  value below  $\sim 250$  K (Figure 4).

There is no evidence of thermal hysteresis in these experiments. The same  $Q_H(T)$  curves, within experimental precision, were obtained whether the corresponding temperatures were reached along cooling or warming sequences. The same  $Q_H$  values were recovered  $>60$  min after the frozen solutions had reached thermal equilibrium. Because reactions (1, -1) are known to exhibit acid catalysis in solution,<sup>33,36</sup> the fact that  $Q_H$ 's measured in frozen acidified solutions are not significantly different (inset, Figure 4) supports the assumption of chemical equilibrium in the frozen state, even at the lowest temperatures. This empirical conclusion is consistent with the relaxation times  $\tau < 100$  s, for approaching equilibrium (1, -1) in aqueous  $[H^+] = 0.1$  M solutions, estimated by extrapolation of available kinetic data to 250 K.<sup>33</sup>

These experiments show that equilibrium (1, -1) is not arrested at the freezing point, but remains dynamic down to significantly lower temperatures, despite the reduced water activity and molecular mobilities prevailing in the unfrozen portion. What prevents the complete dehydration of PAH at lower temperatures? Although  $a_w$  is a function of both  $x_w$  (Figure 3) and temperature in aqueous solutions, the onset of the phase equilibrium:  $H_2O(l, x_w) \rightleftharpoons H_2O(s)$ , renders  $a_w$  an exclusive function of  $T$  below  $T_f$ , independent of the nature of the solute.<sup>48</sup> The activity of water in equilibrium with ice at  $T \leq T_f$  can be evaluated from:<sup>14,15</sup>

$$a_w = \exp \left[ \frac{\Delta H_M}{R} \left( \frac{1}{T_f} - \frac{1}{T} \right) \right] \quad (3)$$

where  $\Delta H_M$  is the enthalpy of ice melting. Equation 3 leads, with  $\Delta H_M(H_2O) = 6.01$  kJ mol<sup>-1</sup>, to  $a_w = 0.78$  vs the experimental value for supercooled water  $a_w = 0.80$  at 250 K.<sup>49,50</sup> The inverse temperature dependence of  $Q_H$  in 0.1 M PA at  $T > T_f$  is retrieved from eq 2 with  $\Delta H_H = -27.3$  kJ mol<sup>-1</sup>,  $a_w \approx 1$ :  $Q_H = K_H a_w^n \propto \exp [-(\Delta H_H/RT)] = \exp(3621/T)$ . On the other hand,  $n$  may be still approximated by  $n_1 \approx 7$  just below  $T_f$ , but now  $a_w$  is given by eq 3 with  $\Delta H_M(D_2O) = 6.34$  kJ mol<sup>-1</sup>. The expression that follows:  $Q_H \propto \exp [-(\Delta H_H + n_1 \Delta H_M)/RT] = \exp[-2062/T]$ , correctly predicts the reversal of  $\partial Q_H / \partial T$  about  $T_f$  (Figure 4). In contrast with the thermal behavior of the 0.1 M PA solution, the monotonic increase of  $Q_H$  upon cooling the 4.64 M PA solution, even below its corresponding freezing point (Figure 4), implies that in this case:  $\Delta H_H + n \Delta H_M \leq 0$ . Thus, PA may become more or less hydrated in the frozen state, depending on the initial concentration of the fluid solution. Because  $\Delta C_{p,m} \approx 0$ , i.e.,  $\Delta H_M$  is nearly independent of temperature, the thermal behaviors of  $Q_H$  below  $T_f$  depend on the relative values of  $\Delta H_H/n$  and  $\Delta H_M$ .

The experimental observation that  $\partial Q_H / \partial T \rightarrow 0$  as  $T \rightarrow 250$  K for all solutions reflects, therefore, a thermodynamic rather

(48) Koop, T. *Bull. Chem. Soc. Jpn.* **2002**, 75, 2587.

(49) Johari, G. P.; Fleissner, G.; Hallbrucker, A.; Mayer, E. *J. Phys. Chem.* **1994**, 98, 4719.

(50) Koop, T.; Luo, B.; Tsias, A.; Peter, T. *Nature* **2000**, 406, 611.

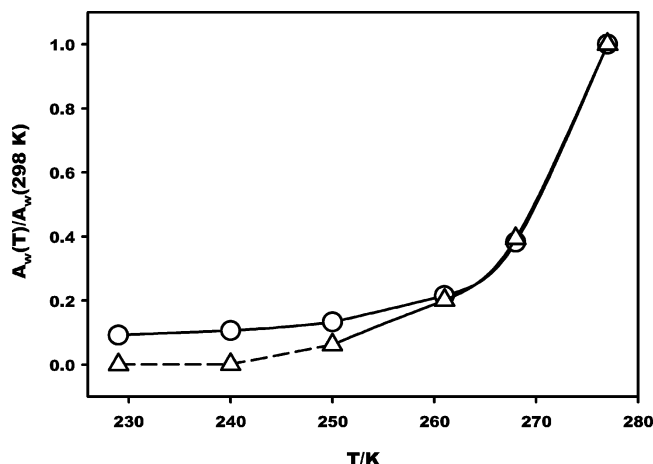


**Figure 5.** Integral intensity of the  $1\delta > 5$  ppm water signals as function of temperature. ( $\Delta$ ) in 0.10 M PA. ( $\circ$ ) in 0.16 M PA/0.13 M HCl.

than a kinetic condition: it actually requires that  $(\Delta H_H + n\Delta H_M) \rightarrow 0$  in the presence of ice at low temperatures. The data of Figure 3 suggest that  $n$  is likely to decrease along with temperature in the increasingly concentrated solutions remaining below  $T_f$ . By assuming that  $\Delta H_H \rightarrow 21.3$  kJ mol $^{-1}$  at low temperatures (as for the 2.32 M PA solution that leads to  $Q_H = 4.0$  at the onset of freezing) we arrive at the conclusion that a minimum of  $n \sim 3.5 \pm 0.3$  water molecules are needed to hydrate the carbonyl group of PA in ice below  $\sim 255$  K. This figure provides a stringent measure of hydrogen  $\sigma$ -bond cooperativity as a mechanistic requisite for solute hydration under rather adverse conditions.<sup>2,36,39,51–53</sup>

The preceding evidence suggests that PA hydration occurs in a fluid medium down to, at least, 250 K. A rigid reaction medium would have otherwise restricted the expansion ( $\Delta V_1 = -5 \times 10^{-3}$  L mol $^{-1}$ )<sup>54</sup> associated with PAH dehydration. Because the area of the  $1\delta > 5$  ppm signals of Figure 2,  $A_w$ , gauges the amount of liquid water in frozen solutions,<sup>9,43</sup> and  $A_w$  vanishes below  $\sim 250$  K (Figure 5), water seems to freeze completely at the point at which  $Q_H$  becomes independent of

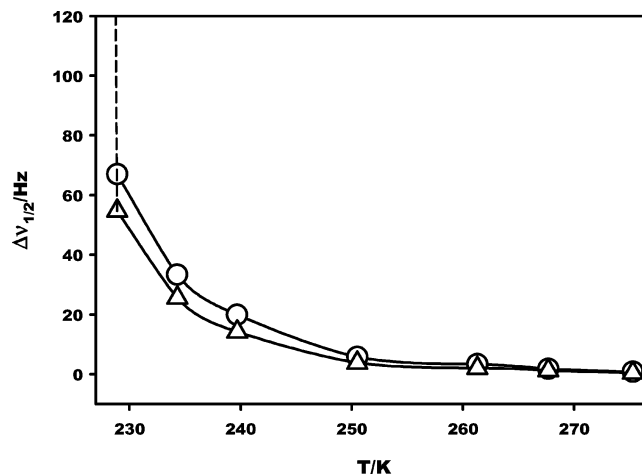


**Figure 6.** ( $\circ$ )  $1\delta: \approx 2.4$  ppm and ( $\Delta$ )  $\sim 1.5$  ppm signal line widths at half-height as function of temperature in frozen 0.1 M PA in D $_2$ O.

temperature. On the other hand, the line widths of methyl proton resonances, which gradually increase at lower temperatures (Figure 6), abruptly broaden below  $\sim 230$  K (i.e., about 20 K below the disappearance of mobile water) as an indication that internal rotations of methyl groups become too slow to effectively average local magnetic anisotropy,<sup>55,56</sup> at temperatures that are commensurate with the glass transition of bulk supercooled D $_2$ O,  $T_g = 233$  K.<sup>19,57</sup> DSC thermograms of frozen PA solutions, which display a single endotherm at the onset of ice melting (Supporting Information), further confirm that PA aqueous solutions freeze into ice and a fluid solution that eventually vitrifies at  $\sim 230$  K.

**Acknowledgment.** L.H. was a SURF student. The present study is supported by the National Science Foundation under grant number NSF-ATM-0228140. We thank Sonjong Hwang, and Peter Babilo, for technical support.

**Supporting Information Available:** DSC endotherms obtained upon warming frozen pyruvic acid solutions in D $_2$ O. This material is available free of charge via the Internet at <http://pubs.acs.org>.

JA062039V

- (51) Steiner, T. *Angew. Chem., Int. Ed.* **2002**, *41*, 48.
- (52) Collins, M. D.; Hummer, G.; Quillin, M. L.; Mathews, B. W.; Gruner, S. M. *Proc. Natl. Acad. Sci. U.S.A.* **2005**, *102*, 16668.
- (53) Dashnau, J. L.; Sharp, K. A.; Vanderkooi, J. M. *J. Phys. Chem. B* **2005**, *109*, 24152.
- (54) Agreiter, J.; Frankowski, M.; Bondybey, V. *Low-Temperature Physics* **2001**, *27*, 890.

- (55) Gutowsky, H. S.; Holm, C. H. *J. Chem. Phys.* **1956**, *25*, 1228.
- (56) Krishnan, V. V.; Lau, E. Y.; Tsvetkova, N. M.; Feeney, R. E.; Fink, W. H.; Yeh, Y. *J. Chem. Phys.* **2005**, *123*, 044702.
- (57) Skaliky, J. J.; Sukuruman, D. K.; Mills, J. L.; Szyperski, T. *J. Am. Chem. Soc.* **2000**, *122*, 3230.